REMOTE SENSING FOR AGRICULTURAL WATER MANAGEMENT

Assignment: Part 2

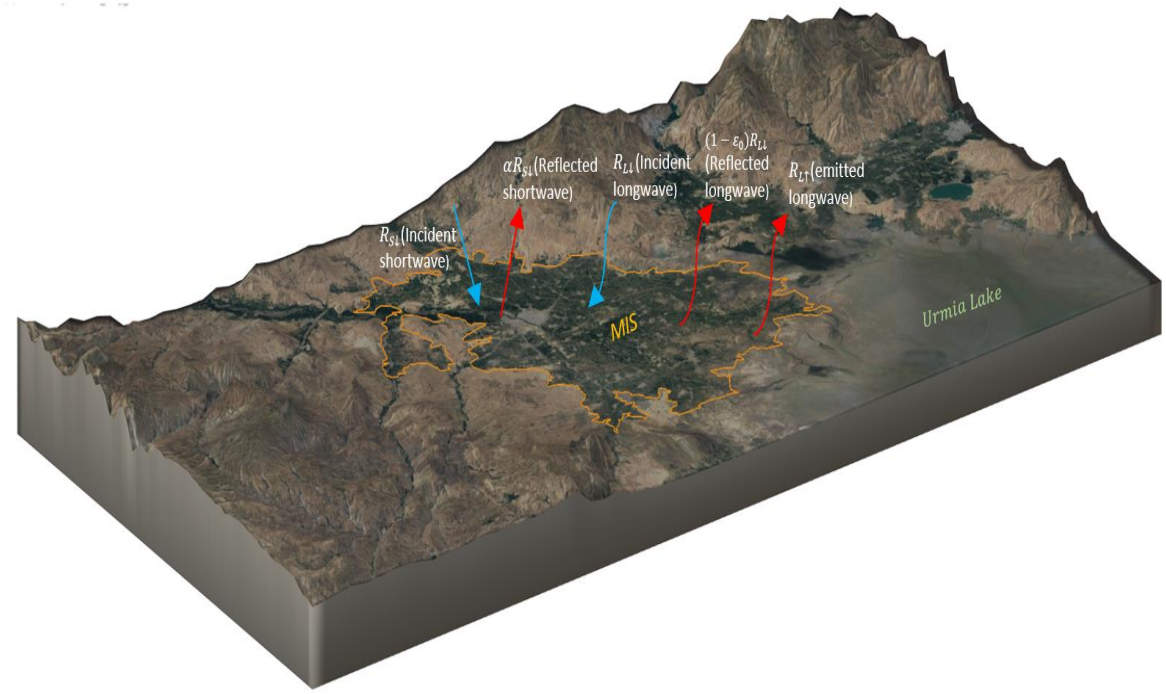

Presented to

Poolad Karimi

Sajid Pareeth

Submitted by: **Group 1**

Aditya Vikram Jain

Zhang Fengbo

Luis Felipe Sierra Ponguta

Sintayehu Fetene Demessie

Kiggundu Hadar

Natalia Cárdenas Niño

Juan Bernal

UNESCO IHE DELFT

DELFT, NETHERLANDS

2020

Contents

List of Figure

List of Table

1. INTRODUCTION

1.1 Evapotranspiration

Evapotranspiration is a combination of both evaporation and plant transpiration where water is lost from the earths land surface, plant surface and water surface to the atmosphere. Evaporation accounts for movement of water to the atmosphere from surfaces like soil, plant canopy interception and water bodies and on the other hand transpiration accounts for subsequent loss of water inform of vapor through the leaves stomata openings. Evapotranspiration is significantly affected by the type of vegetation, land use, climatic factors, environment and management aspects. Both process require energy inform of solar radiation to occur.

1.2 Biomass

Biomass is a form of renewable energy which accounts for the total amount of organic matter in a given area or population. Biomass production is expressed in two forms i.e. primary production which involves generation of energy by plants through the process of photosynthesis and secondary production which refers to absorption of organic matter inform of body tissues by organisms.

1.3 Remote Sensing

The use of remote sensing techniques to determine the spatiotemporal distribution of evapotranspiration and estimation of biomass production on a large scale can be of a grate paramount to provide information such as estimating the seasonal and annual consumptive water use and planning. This study aims at using the surface energy balance algorithm for land (SABEL) model to map seasonal and annual ET, biomass production and creating seasonal NDVI maps in MIS by processing single individual images and gap filling. It also aims at conducting crop type based analysis of ET and biomass production for a period of four crop years (2015/2016-2018/19).

1.4 Study area

This case study is in Urmia basin in Iran, Lake Urmia is an endorheric salt and the largest lake in the Middle East that is located between the East Azerbaijan, the western Azerbaijan provinces and the southern part of the Caspian Sea. The lake covers a surface area of approx. 5,200km2 and a maximum depth of 16m (https://en.wikipedia.org/wiki/Lake_Urmia). Studies show that more than 6.5million people in the Urmia basin depend on agriculture and industry as the major sector(*Bakhshianlamouki et al.*, 2020). There is intensive irrigation agriculture systems in the basin using river canals and pressurised ground water systems which are a major sources of livelihood and food security for the farmers (*Hesami and Amini*, 2016). However, these agricultural activities, damming of the local rivers, and ground water abstraction in the basin have caused the reduction in the inflows to the lake and have caused the shrinkage of the lake(*Bakhshianlamouki et al.*, 2020).

The Miandoab irrigation scheme (MIS) is a major irrigation scheme in the Urmia basin which is of a great importance to food security, however as a measure to restore the Lake, the government of Iran decided to reduce the irrigation water allocated to the scheme by 40% by increasing the performance of the scheme without causing a negative impact on food production. The scheme has two major cropping seasons (the winter and the summer) with a crop year from October to September next year. The major crops grown in the scheme are wheat, barley, vegetables, orchards and Alfalfa among others.

2. METHODOLOGY

2.1 General workflow

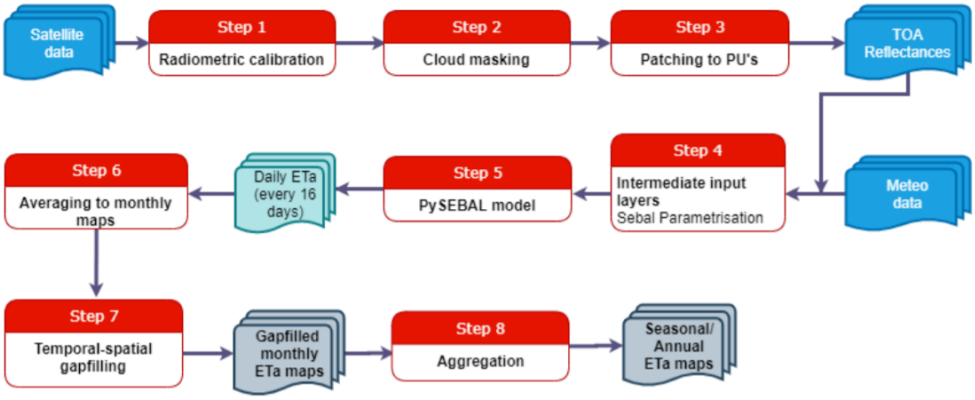

Figure 1 *General workflow diagram (source: from slides in class)*

The General workflow diagram is shown in figure 1. Satellite images from Sentinel 2 were downloaded for 2018/19 seasonal year and combined with the digital elevation model for MIS, metrological and soil data and the surface energy balance algorithm for land (SEBAL) was applied to determine the evapotranspiration, biomass and the normalised difference vegetation index (NDVI) corresponding for each Sentinel imagery date of acquisition.

The daily maps obtained were then converted to monthly since the satellite has a temporal resolution of 16 days. Spatial gap filling was done by applying the time series interpolation algorithm and then the monthly maps were aggregated to seasonal and annual.

2.2 Satellite data and field data

PySEBAL library requires spatial data in raster format to calculate Eta. This model has been tested mostly with Landsat 7 and 8 images, as is the case of this exercise. The model uses information from Bands 1 – 5 and 7, which are associated with visible data and near-infrared, and band 6 which has thermal data. This data needs to be clear and without clouds otherwise need to be gapfilled.

Soil data related to moisture content in soil and field capacity is also required and is obtained from HiHydroSoil database. Meteorological data is obtained from the NASA Global Land Data Assimilation System (GLDAS) and is composed from Temperature, humidity, windspeed and

radiation shortwave data. In the table below are shown the base data sets needed to compute PySebal.

Table 1 *Data require for the PySEBAL computation*

SATELLITE IMAGERY	METEOROLOGICAL DATA	SOIL DATA
Landsat 8 Images Bands 1 - 7	Instantaneous Temperature	Saturated soil moisture content
	24-Hr temperature	Saturated soil moisture content subsoil
	Relative Humidity Instantaneous	Residual soil moisture content
	Relative Humidity 24 Hr	Residual soil moisture content subsoil
	Wind Speed Instantaneous	Field Capacity
	Wind Speed 24 Hr	Wilting point

2.3 Surface energy balance and PySEBAL introduction

The evapotranspiration (ET) is a parameter linked to vapor water losses in the hydrological cycle, and it cannot be seen. The measure of ET is carried out with lysimeters, which are located on the ground and represent local measures in the basin. Due to the influence of a combination spatiotemporal of different atmospheric, plant, and ground components, ET is a parameter complicated to calculate at the basin level.

SEBAL (*Bastiaanssen et al.*, 1998) is an empirical algorithm that uses visible and thermal infrared spectral radiance from satellite imagery to compute ET flux spatially at basin level in time. The ET as residual from the surface energy budget equation flux is computed at pixel image resolution using the following formula.

$$\lambda ET = R_n - G - H$$

Where:

λET*: Latent heat flux (W/m²)*

R_n*: Net radiation flux at the surface (W/m²)*

G*: Soil heat flux (W/m²)*

H*: Sensible heat flux to the air (W/m²)*

The energy budget equation requires information from the soil, atmosphere and coverage to be computed. The net radiation flux at the surface parameter depends on the shortwave and longwave radiation to be computed. In the figure below is shown the atmospheric components that affect the energy budget equation.

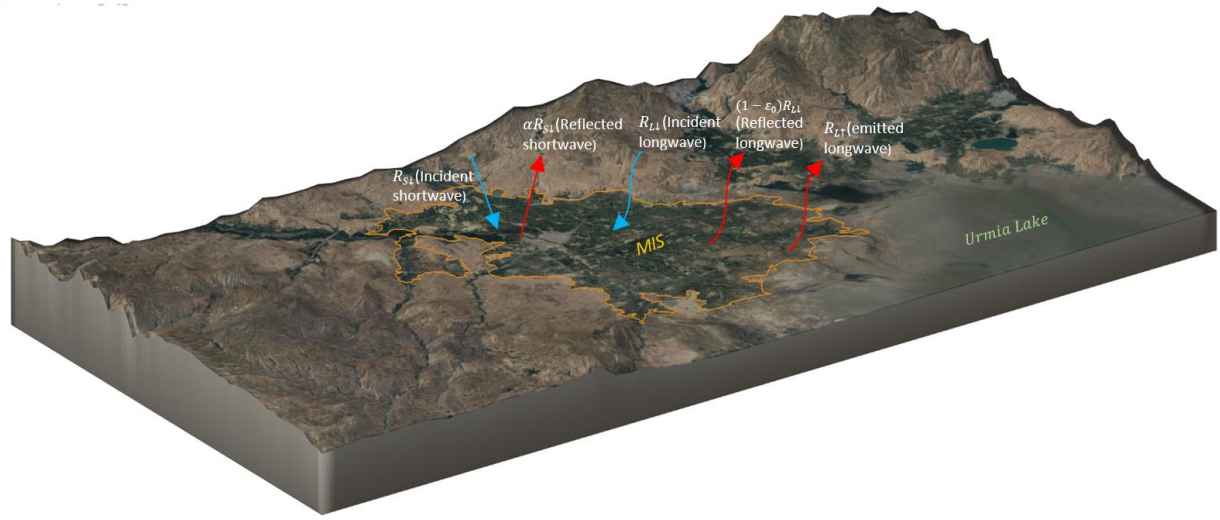

Figure 2 *Atmospheric components in the energy budget equation*

From Figure 2, the net radiation flux is calculated as follows.

$$R_n = R_{S\downarrow} - \alpha R_{S\downarrow} + R_{L\downarrow} - R_{L\uparrow} - (1-\varepsilon_0)R_{L\downarrow}$$

Where $\propto$ is the surface albedo, and ε_0 is the surface emissivity. ε_0 is calculated as

$$\varepsilon_0 = 1.009 + 0.047 * \log(NDVI)$$

The parameters used by SEBAL algorithm are the hemispherical surface reflectance r_0, NDVI index surface temperature $R_{L\downarrow}$ which is computed as follows.

$$R_{L\downarrow} = \varepsilon_a \sigma {T^4}_i \qquad R_{L\uparrow} = \varepsilon_a \sigma {T^4}_s$$

$$\varepsilon_a = 0.85(-ln\tau_{sw})^{0.09} \qquad \tau_{sw} = 0.75 + 2x10^{-5}$$

Where ε_a is the atmospheric emissivity, σ is the Stefan-Bolztman constant and T_i is the incident near-surface air temperature

PySEBAL is a library widely tested on Landsat 7 and 8 imageries that can compute Actual Evapotranspiration (Eta) applying the SEBAL algorithm. Other capabilities from this library are computations of water productivity on biomass. In the figure below is shown the SEBAL algorithm conceptual scheme. The conceptual scheme of the budget equation flux computed by SEBAL is shown in the figure below.

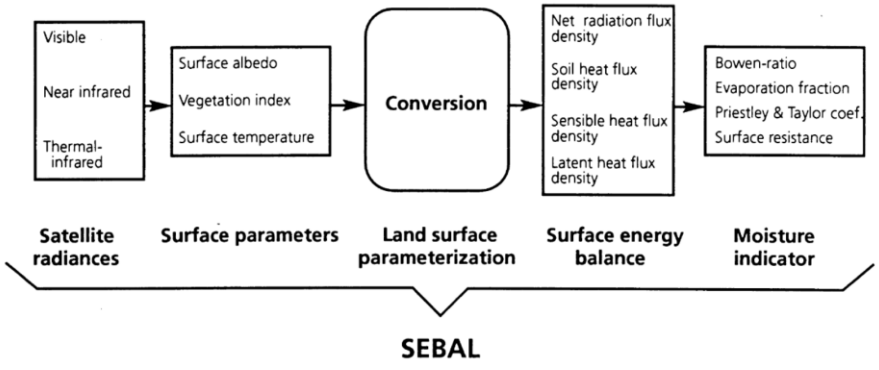

Figure 3 *Conceptual scheme SEBAL algorithm (Bastiansen-1998)*

The result of applying the SEBAL methodology using PySEBAL is a set of raster files for the area of interest, which is defined by the DEM domain. These files are divided into three main groups Biomass production, evapotranspiration, and vegetation. The cloud presence in some images makes it necessary to do other analyses to complement the regions with wrong data values.

Crop biomass production is obtained from photosynthetically active radiation (PAR) raster data. APAR, which is a fraction of PAR is the active radiation absorbed by the canopy and used for carbon dioxide assimilation (*Grosso et al.*, 2018). The biomass production is computed from a single image using the formula below.

$$bio = e'.\Lambda.fPAR.0.84$$

Where,

e': Light use efficiency

Λ: Water stress index

$fPAR = -0.161 + 1.257.NDVI$, is the APAR/PAR fraction estimated from NDVI index

2.4 Temporal-spatial Gapfilling

Gap-filling is used when the presence of clouds in the images produce wrong ETa data patches. There are four steps for gap-filling images that are summarised below:

- Averaging and multiply rasters: Landsat satellite only takes 2 images each month. In order to have rasters each day, the image results are averaged and multiplied by the number of days in a month.
- Temporal interpolation: A locally weighted regression of time series is used to estimate missing values and outliers by using a polynomial function constructed with neighbouring time values.
- Spatial interpolation: No data values in a raster are filled using spline interpolation, and the fill areas are interpolated from the boundaries with no data.
- Filtering: A final step to remove any remaining outliers is carried out to the raster output data.

3. RESULTS

3.1 Evapotranspiration

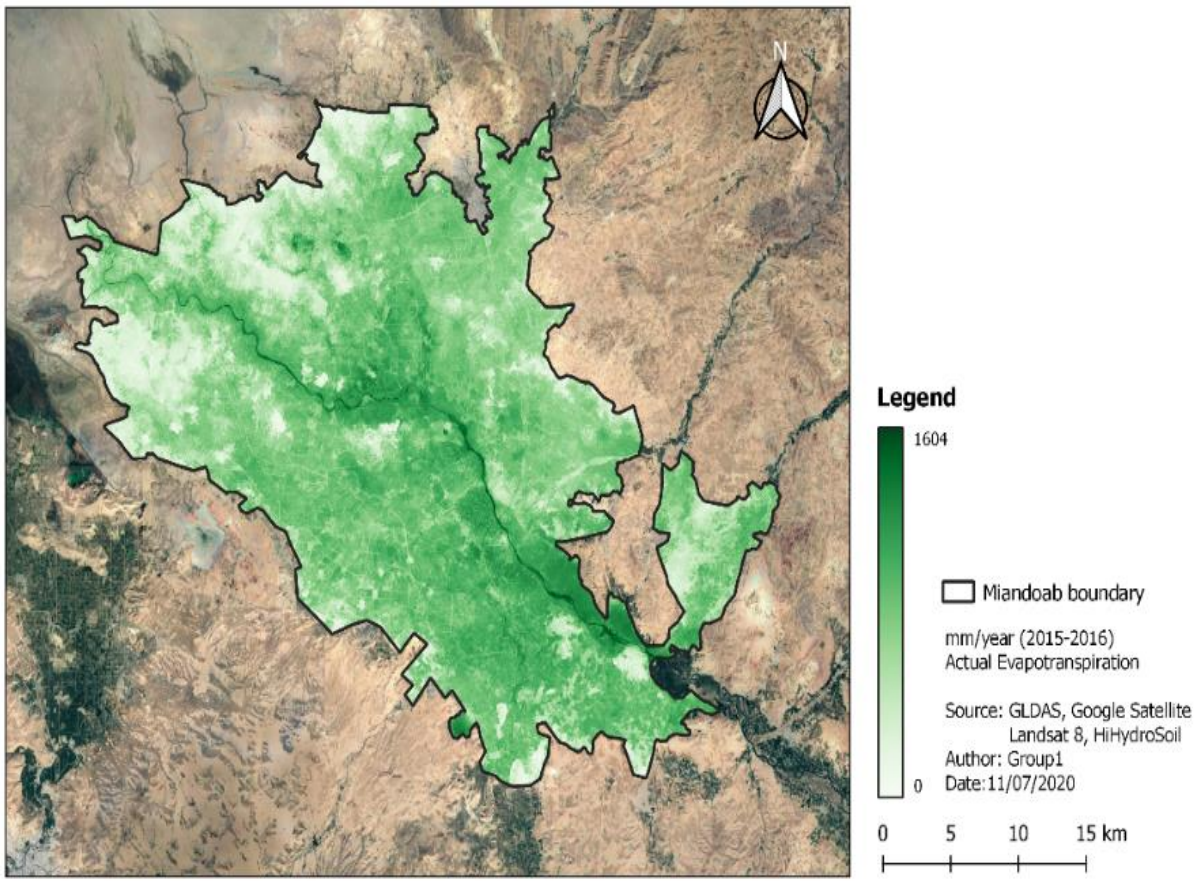

Figure 4 *Evapotranspiration annual scale map*

The ETa annual distribution for the study period in MIS is shown in Figure 4. The average range obtained is between zero and 1604 mm/a, the main values are located at SouthEast of the basin and along the Zarrine River. Near the Lake Urmia shore, it can be observed without places where the ETa es closest to zero, and these places likely match with salinisation and desertification process closest to the lake. There are other places in the basin where exist bared soils which have low evapotranspiration rates.

Urmia Basin exists a crop calendar which depends on meteorological conditions, as shown in figure 12. The winter crops like wheat and barley with an annual ETa of 812 mm, shows the following ETa distribution along the cropping year; S1=13.7%, S2=10.2%, S3=30.7 and S4=45.4%.A summer crop like the Sugarbeet with 837.12 mm of ETa for all its crop cycle, split the ETa like follows; S1=11.7%, S2=6.3%, S3=32% and S4=50%. An annual crop like Alfalfa has the next ETa percentage behaviour S1= 11.2%, S2=3.2%, S3=31.6 and 49.4%. Overall, using the r.stats. Zonal tool of QGIS, it was found for this study period and for any crop, that ETa distribution average was for S1=12%, S2=8%, S3=31% and S4=47.6%. Figure 5 shows the trend of ETa distribution by season, which match with that described for the mentioned crops.

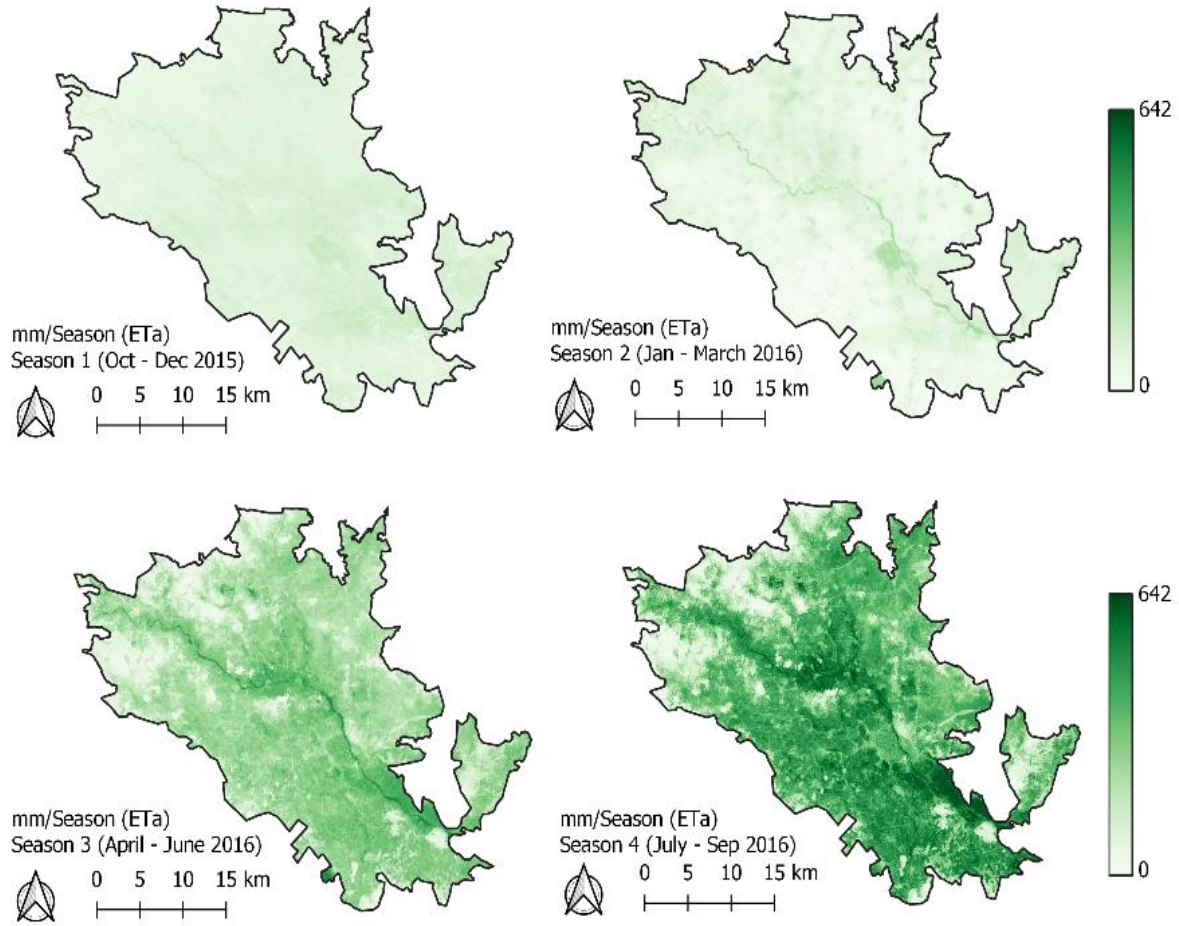

Figure 5 Seasonal Eta map

Figure 6 shows the time series of ETa and P over eight different crops from October 2015 to September 2016. The rainfall during the first semester (139.9mm) was greater than the second (23.9 mm)(*WWO*, 2020), It reflects in the ETa behaviour with higher peaks in summertime when precipitation is lowest or even zero like in this period, and temperatures rise. During the period November- February ETa average for all crops show values under 25 mm/month, this is the same period of winter crops like wheat and barley. From March to August there is an ETa rising, with a sharp peak in July. The crops with main water consumption in the second cropping semester were the apple and pears (212 mm/month); other crops (186 mm/month); Sugar Beet (172 mm/month); Fall Irrigated Vegetables and Alfalfa (156 mm/month) and Grapes (139 mm/month). The Wheat and Barley crops present the lower ETa average peak with 108 mm/month.

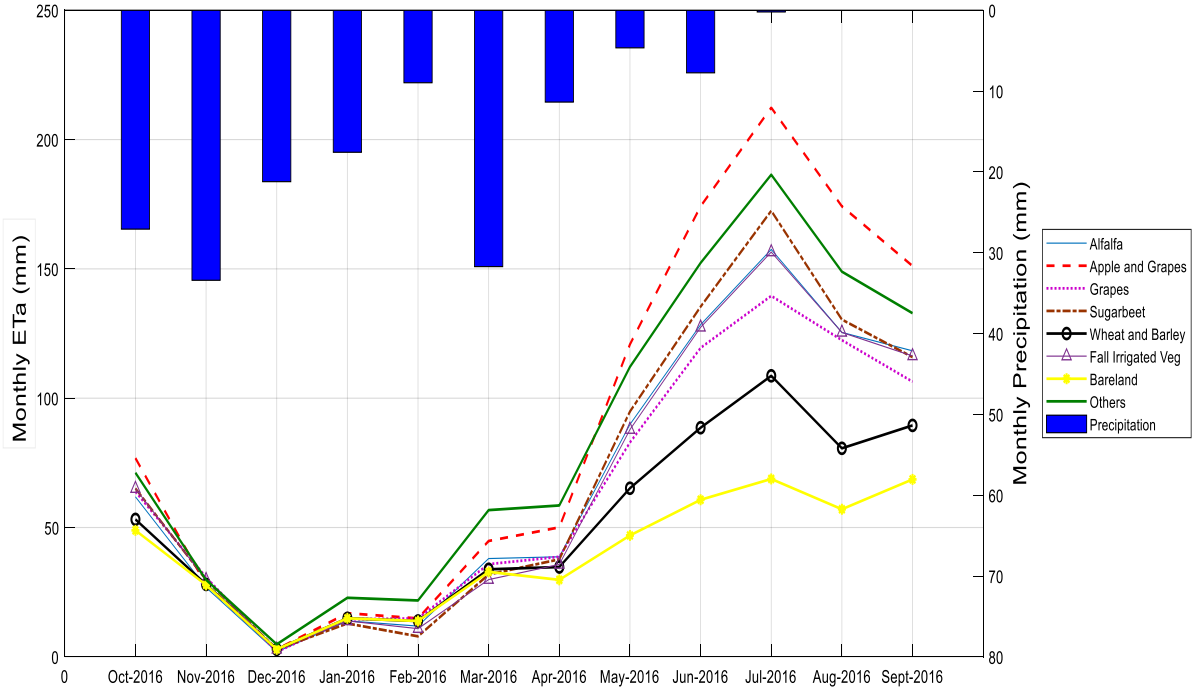

Figure 6 *ETa trend by land cover*

3.2 Normalised Difference Vegetation Index – NDVI

The NDVI mean the annual map is presented in Figure 7, in which the scale rate goes between 0 to 1, being cero the lowest NDVI value and 1 the value of a full and healthy vegetated area. The Miandoab Irrigation Scheme characterised for being an agricultural region, has crops as the highest land cover, the reason why the values of the NDVI in most of the maps tend to be in the middle of the scale rate of this index. Also, it can be seen that the places with the lowest values correspond to the city that is in the middle of the map (builtup), bareland as the one near to the Urmia Lake, and small water bodies as lakes or the river.

Figure 8 shows the changes in the NDVI over time. Season 1 (October to December 2015) corresponds to the winter season in the study area, the reason why the NDVI values, in general, are really low. In season 2 (January to March 2016), the winter keeps affecting the crops and the vegetation, so again the values of the NDVI, in general, are low. Then, in season 3, which occurred a transition between the winter season and the summer season, the NDVI values increased, showing that the vegetation of the region started growing. Finally, season 4 that coincided with the summer season is the one with the highest NDVI values, in which the climate provides optimal conditions for the growth of vegetation, as agriculture.

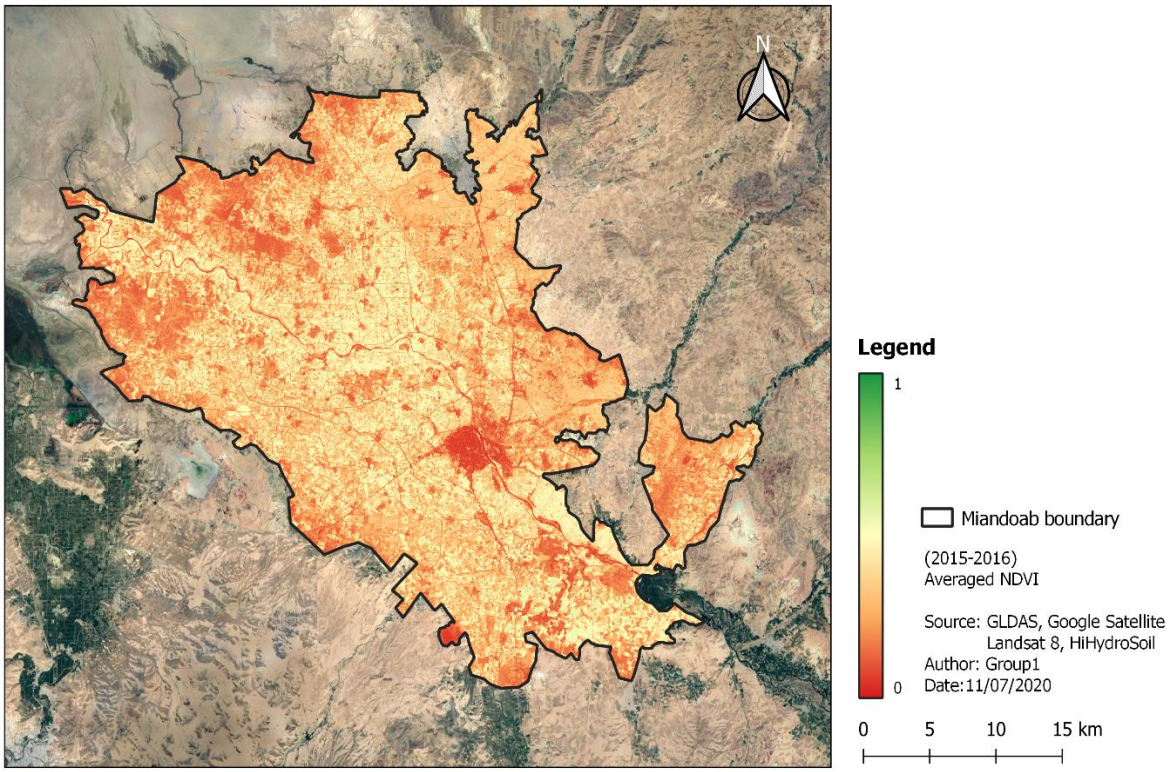

Figure 7 *NDVI annual scale map*

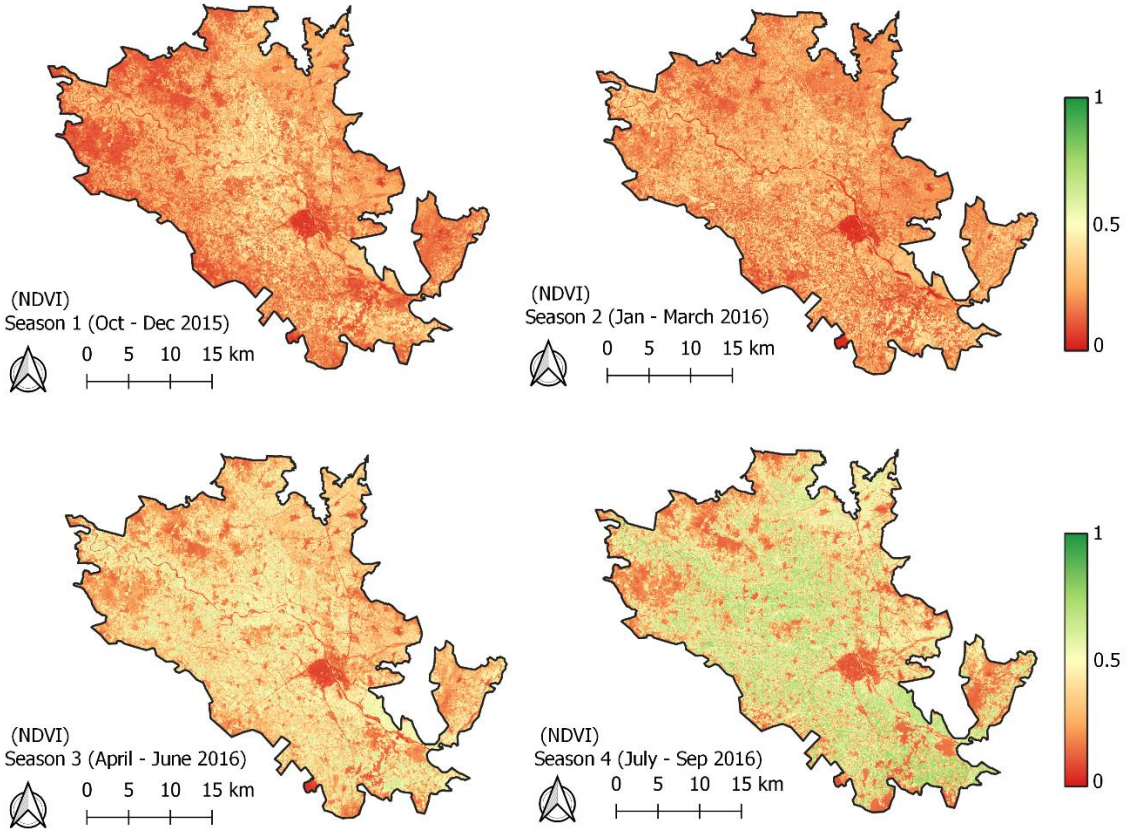

Figure 8 *Seasonal NDVI map*

In general, the trend of the NDVI, shown in Figure 9, for all the crops corresponds to the trend of the climate seasonality of the study area, in which the first two seasons, winter season, presented the lowest values of NDVI for each crop. In season 3, in the transition between winter season and summer season, the value of the index starts increasing in all the crops. Finally, season 4 that corresponds to the summer cropping season, in which most of the crops are in their growing or harvesting stage, presented a higher canopy area. Hence, the values of the NDVI by detecting more vegetated cover are going to be higher than in the rest of the seasons.

Moreover, the crop or crops with the highest NDVI value were the apple and pear crop that reported the highest value of NDVI during all seasons, presenting the highest value during season 4 with 0.65, this could be due to the type of crop because these crops types are characterised for being trees that remain during all the seasons. The alfalfa crop was the second one presenting a high value of the NDVI, compering to the rest of the crops, with an index that fluctuated between 0.28 and 0.54. The rest of the crops reported the same trend with similar values for the NDVI.

It can be seen that the parameter "Other" includes vegetation due to the NDVI calculation shows values between 0.26 and 0.5, and this can be the native vegetation of the region along the river. Lastly, as it was expected the land covers with the lowest values were water, Builtup and Bareland, due it does not have vegetation. Hence, the value of the NDVI has to be near to zero or below.

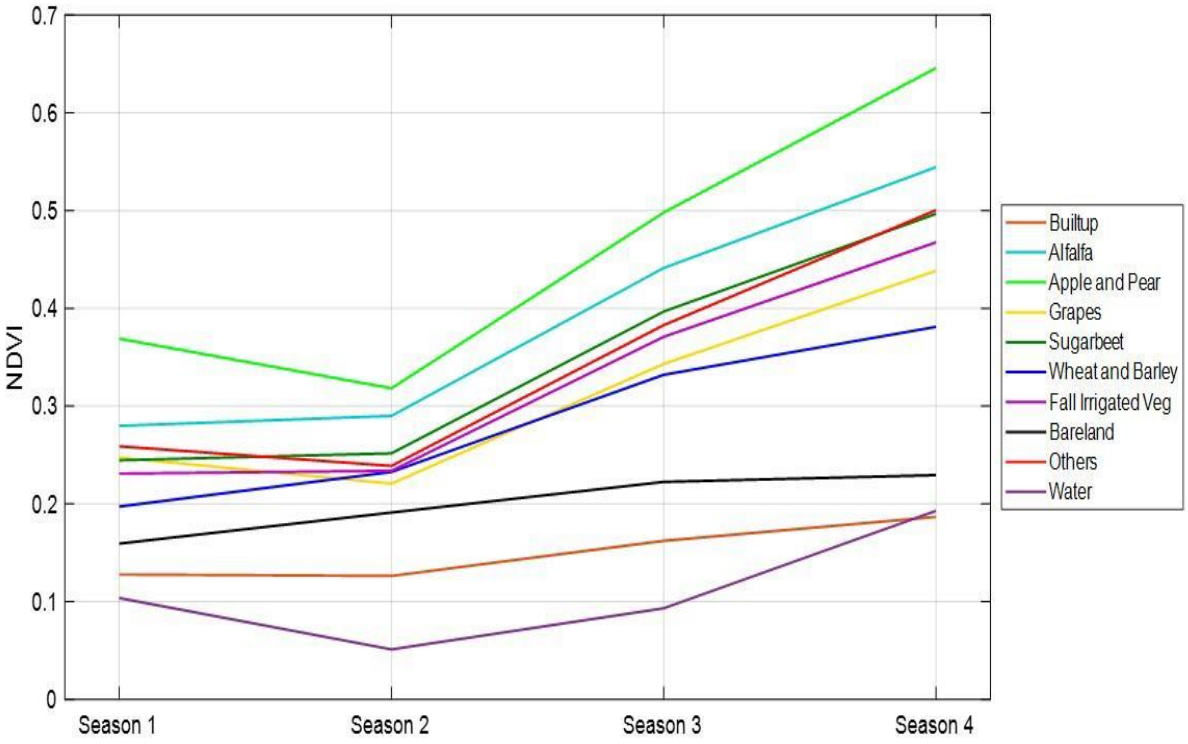

Figure 9 *NDVI of the land cover of MIS during the 4 season*

3.3 Biomass production

Biomass denotes all the living mass of above ground as well as below ground sections of crops, trees, roots and shrubs. It also includes the dried or destroyed coarse or fine litter associated with the soil. In this paper, the biomass production as mass per unit area (kg/ha). The below Figure 10 depicts the monthly and seasonal biomass production in the study area of MIS.

As it can be seen from the figure in the first season (October – December 2015), the minimum biomass of 1727 kg/ha/season in Apple and Pear area, which has maximum biomass productions in all type of land cover, was recorded as compared to the other seasons in the area, as shown in table 2. This might be related to the dryness conditions of the study area in that particular seasons since biomass has a direct link with the evapotranspiration rate.

Whereas in the last season (July – September 2016) the resulted biomass production in Apple and Pear area was around 9388 kg/ha/season which is the maximum of the whole seasons as compared to the other seasons in the MIS, as shown in table 2. In the area, this season is a crop growing summer season so that much more biomass was produced as expected.

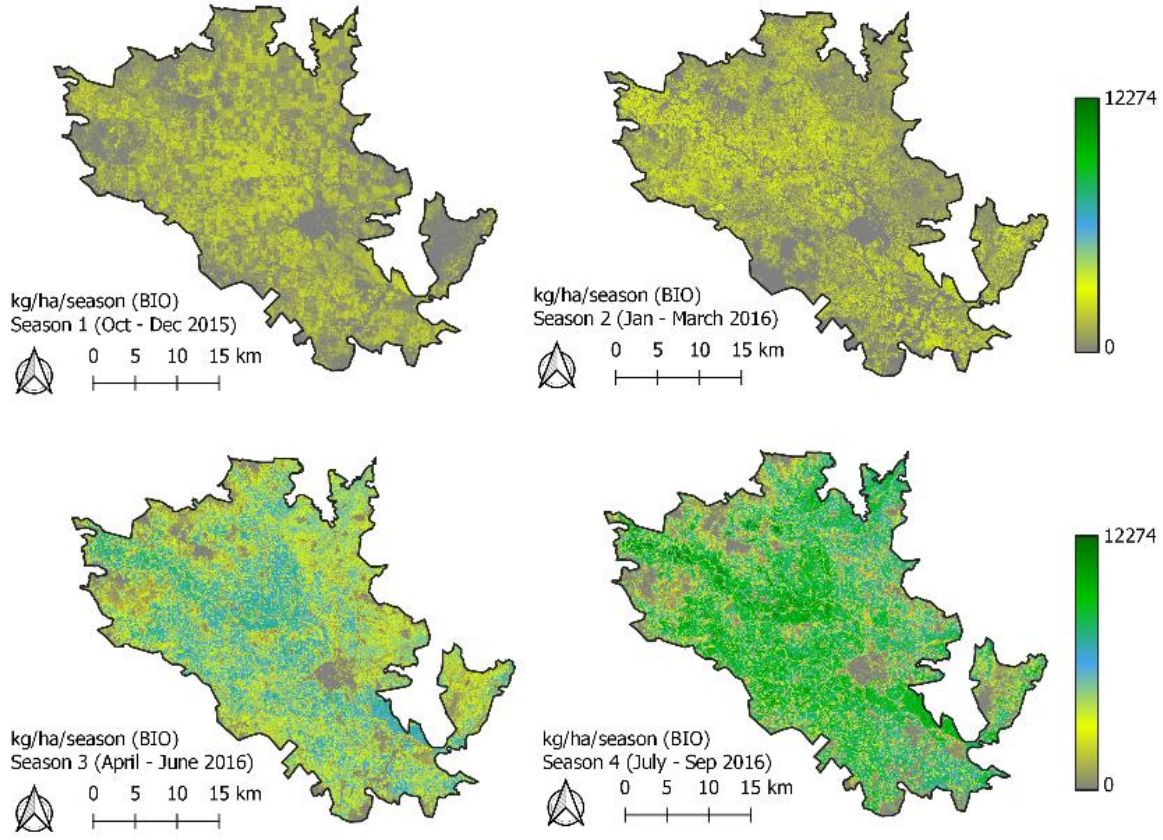

Figure 10 *Seasonal Biomass map*

Table 2 *Biomass of the land cover of MIS during the 4 season*

BIO	Season1(kg/ha/season)			Season2(kg/ha/season)			Season3(kg/ha/season)			Season4(kg/ha/season)		
Zone	min	max	mean	min	max	mean	min	max	mean	min	max	mean
Builtup	0	1587	244	0	1787	169	0	5050	760	0	7536	1207
Alfalfa	212	2490	1237	26	2972	1518	1822	7991	4948	1748	10940	6872
Apple and Pear	744	2524	1727	417	2969	1714	4457	8146	6449	7094	11722	9388
Grapes	119	2293	986	31	2719	860	1102	7118	3929	1422	10148	6085
Suger beet	60	2412	1023	0	2972	1096	1173	7536	4173	995	10393	5957
Wheat and Barley	8	2361	764	2	2952	1070	407	7432	3302	113	10321	4409
Fall irrigated vegetable	72	2411	1002	0	2965	978	1003	7672	4122	968	10728	6151
Bareland	0	1930	432	0	2535	607	1	5875	1439	0	8464	1842
Other	60	2499	1192	0	2972	1119	356	7928	4722	447	11773	7095
Water	0	1718	234	0	1259	50	0	4088	676	0	6685	1392

Figure 11 also shows the annually produced biomass production in the MIS. As it is already illustrated in Figure the maximum annual produced biomass was 29,387 kg/ha, and the minimum was 0 kg/ha. For this maximum annual biomass production, the major contributor area is around the North West region and the centre of the MIS near to the Urmia Lake and water body. Significant amounts of biomass production also seen in the South East region of the MIS in the vicinity of the basin called Zarrine. The reason behind the observations of higher values in the above-mentioned areas might be related to the source and availability of water for crop growth. Since much of the irrigated land areas are close to the water body so that the biomass productions also higher as compared to the other land areas a bit far from the water body.

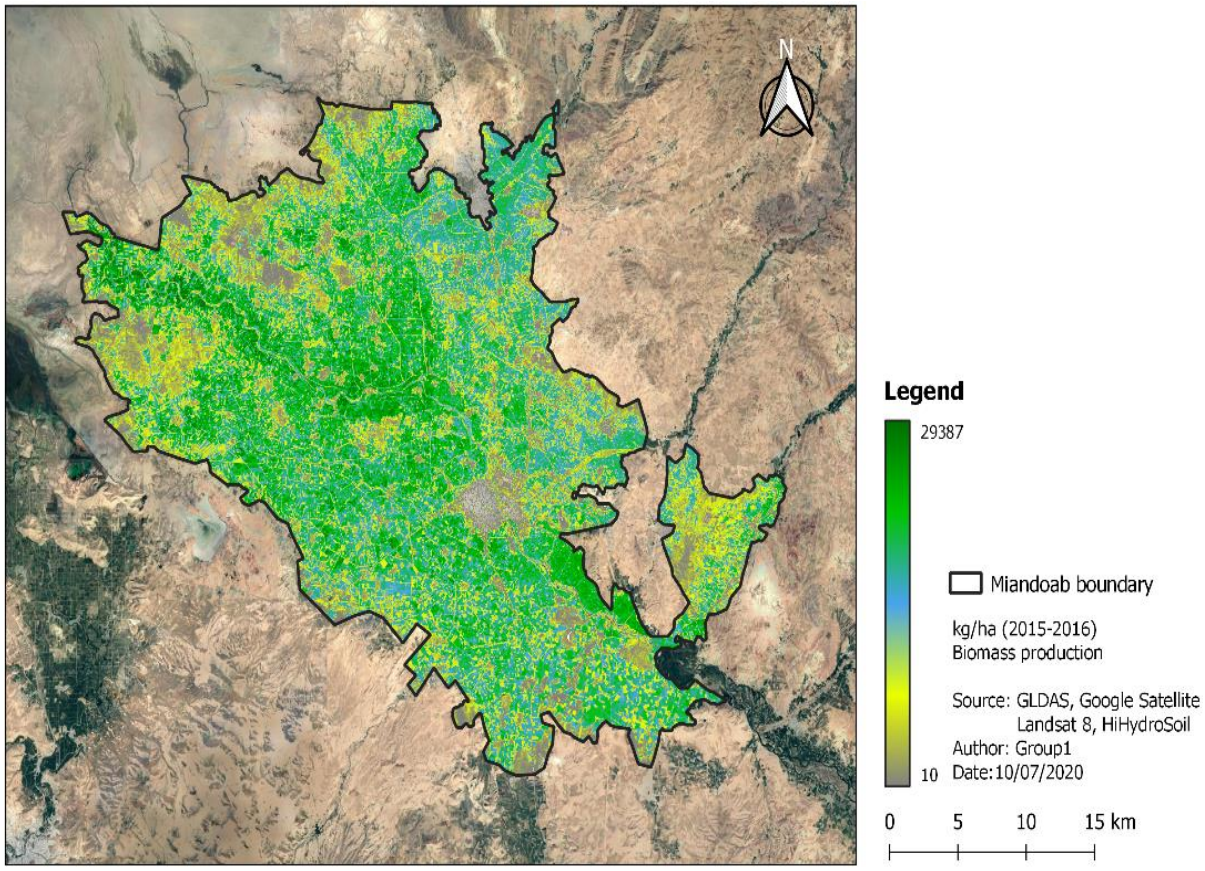

Figure 11 *Biomass annual scale map*

4. DISCUSSION

4.1 Seasonal correlation

Table 3 *Correlation with ETa, BIO, NDVI and TEMP in Season1*

SEASON 1				
	ETA	***BIO***	***NDVI***	***TEMP***
ETA	1			
BIO	0.36	1		
NDVI	0.38	0.99	1	
TEMP	-0.92	0.35	0.35	1

The correlation is quite interesting as some parameters are highly correlated with a value of 99% (NDVI and Biomass). The season one starts with the winter crops and the crops are not in the final stage of development. However, there is so high correlation which can be explained because of all year crops like Apples and pears and Alfalfa.

Table 4 *Correlation with ETa, BIO, NDVI and TEMP in Season2*

SEASON 2				
	ETA	***BIO***	***NDVI***	***TEMP***
ETA	1			
BIO	0.68	1		
NDVI	0.82	0.97	1	
TEMP	-0.99	0.71	0.83	1

The results are different from annual results, the Eta is negatively related to Biomass, NDVI and temperature. The NDVI and temperature is highly correlated. The correlation is comparatively less because of the winter crops which are growing and are not yet developed.

Table 5 *Correlation with ETa, BIO, NDVI and TEMP in Season3*

SEASON 3				
	ETA	***BIO***	***NDVI***	***TEMP***
ETA	1			
BIO	0.23	1		
NDVI	-0.20	0.87	1	
TEMP	-0.72	-0.47	-0.01	1

The biomass is positively correlated to NDVI with 87%. However, the ET is negatively correlated to NDVI and temperature. Due to high seasonal crop in these seasons, the correlation is not so high as in other seasons. The reason can be the development of crop, as it is not in the final stage. So the biomass, NDVI and ET are comparatively less correlated with

each other. In season 3, correlation of ETa and BIO is again low, compared with other seasons, because in april-may is starting the summer crop sowing. For that reason there is no biomass enough to strength the correlation with ETa.

Table 6 *Correlation with ETa, BIO, NDVI and TEMP in Season4*

SEASON 4				
	ETA	***BIO***	***NDVI***	***TEMP***
ETA	1			
BIO	0.76	1		
NDVI	0.73	0.99	1	
TEMP	-0.97	-0.84	-0.82	1

The final season has more clear correlation values. The correlation is very high, and as expected the crops is in the final stage of development. The biomass production is highly positively correlated to NDVI. The ET is also positively correlated to Biomass and NDVI.

4.2 Annual correlation

Table 7 *Correlation with ETa, BIO, NDVI and TEMP*

Annual Correlation				
	ETA	***BIO***	***NDVI***	***TEMP***
ETA	1			
BIO	0.34	1		
NDVI	0.22	0.99	1	
TEMP	-0.96	-0.29	-0.19	1

The results obtained from the above were analysed and correlated annually. As expected, Biomass is highly co-related to NDVI, and the Actual evapotranspiration is highly negatively correlated to the temperature. The other parameters are poorly correlated.

Regression analysis was also performed assuming the biomass as an independent variable and other as the dependent variable. The R square value is very high 0.995, which is again a good indicator of how well these are dependent. However, the Standard error is high.

Table 8 *Regression Statistics*

Regression Statistics	
Multiple R	0.997
R Square	0.995
Adjusted R Square	0.992
Standard Error	503.7
Observations	10.0

In all, it can be concluded that the crops like apples, pears and Alfalfa play a key role in water balance in Miandoab area. Other seasonal crops also play a role in the feedback mechanism. However, there are some assumptions involved which might because of proxies involved.

4.3 Reliable of Land cover map for analysis

The best way to evaluate the statistic of parameters in different land cover is using the land cover map in 2015-2016 crop year. However, the land cover map is not available due to missing data. Actually, the launch of sentinel 2A occurred 23 June, 2015, and the launch of sentinel 2B occurred March 7, 2017. The images form Sentinel 2 are available starting from April 2017. Additionally, the number of images bands increase from 21 to 23 after April 2018, leading to the GEE system cannot work to land cover mapping. Moreover, the accuracy of the map classified by images from Landsat 8 is low, and the land-use changes slightly in several years. Therefore, the land cover map in 2018-2019 crop year was used for the statistic evaluation. Last but not least, the accuracies of the statistical mean, min and max in parameters in water part are low. Because, the classification of the water body in the map is bad that most rivers are identified as 'Others', as shown in figure 13. Also, some accuracy errors in the BIO, NDVI and ETa may cause by that. Furthermore, the min and max values selected are values in 5% and 99% area for increasing the accuracy of the estimation.

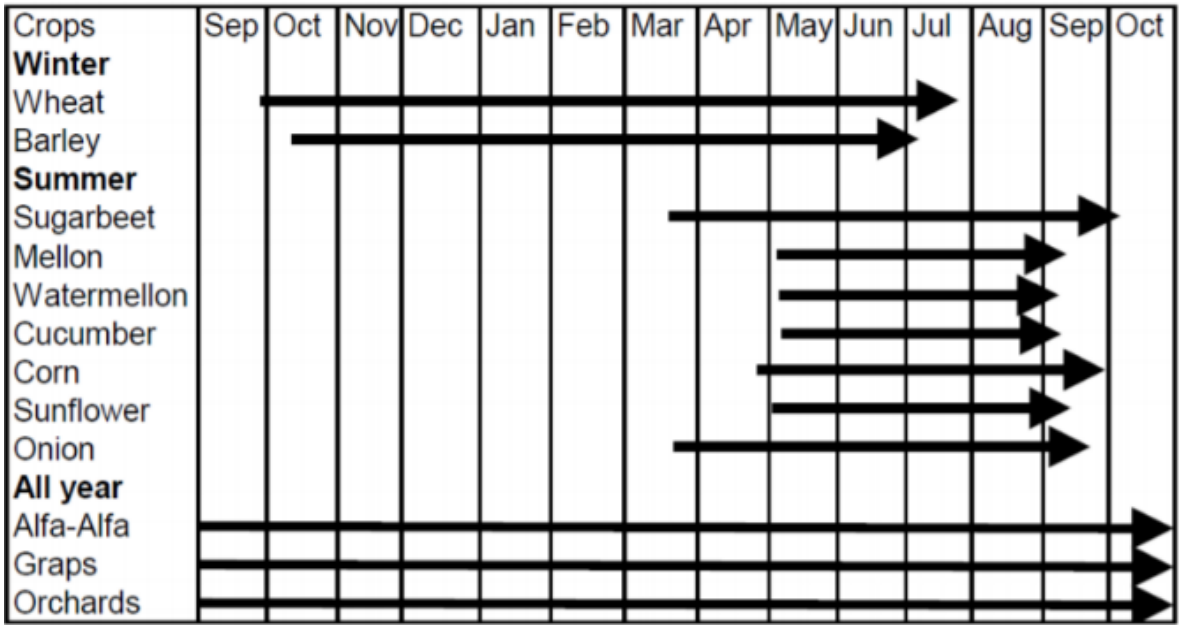

Figure 12 *Typical crop calendar in the region*

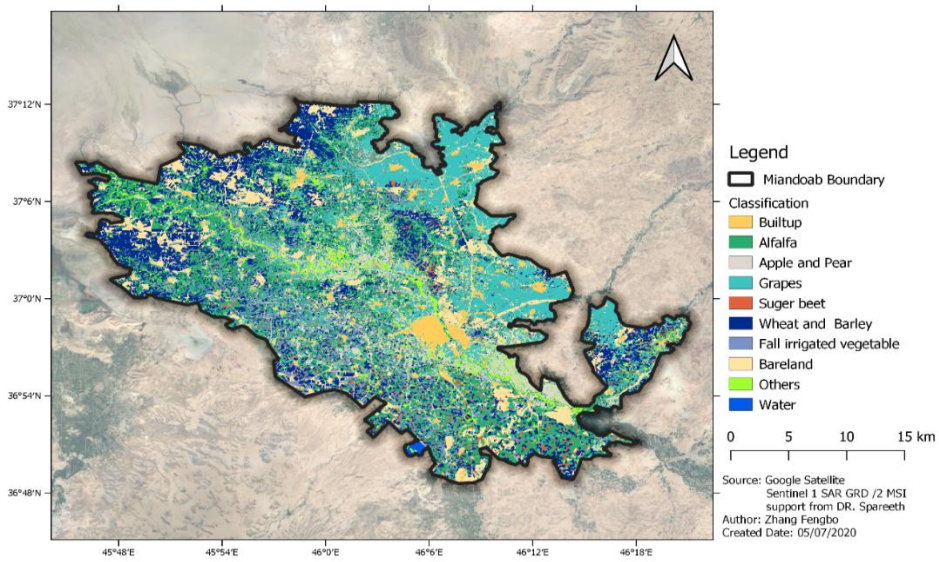

Figure 13 *Land cover map Miandoab Irrigation Scheme 2019*

4.4 Correlation with Precipitation and Actual Evapotranspiration

Figure 6 shows that the evapotranspiration of all types of land is relatively low under 50 mm/month with high monthly averaged precipitation. It may have a relationship with precipitation and actual evapotranspiration. But the only one year data is not enough to prove this relationship, and more data should be analysed for this. Moreover, there are some distributing factors. The period with low evapotranspiration is from October 2015 to April 2016, which is the crop growth stage, and matures crop may have higher transpiration, compared with the growing one. Importantly, temperature also high influence on ETa and the slight variance of ETa caused by the temperature during the period, as shown in Fig 14.

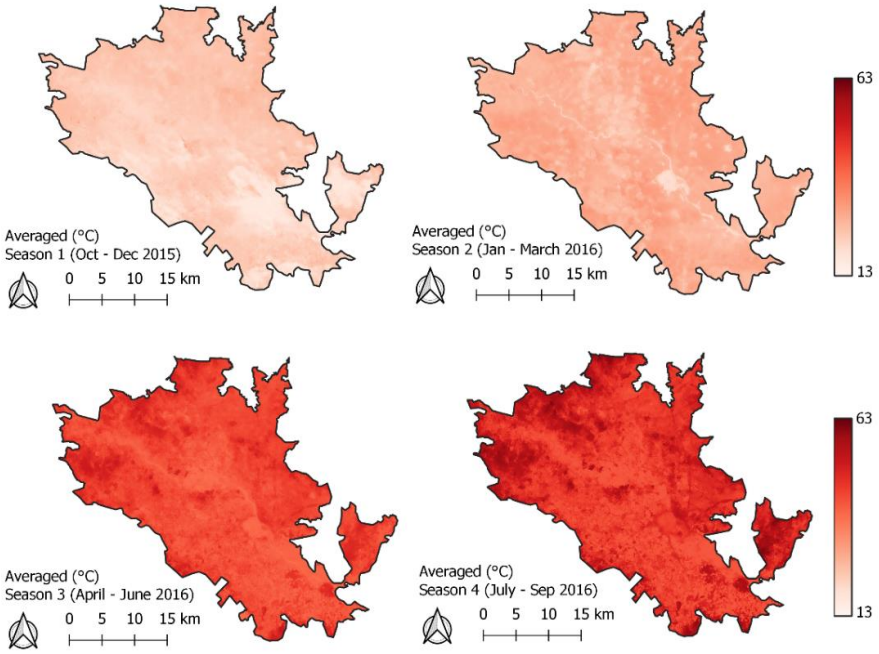

Figure 14 *Seasonal values of Surface temperature in 2015-2016 crop year*

4.5 Biomass estimation in Builtup area

Strangely, the biomass production appeared in Builtup area, as shown in table 2. Because the urban area with a huge number of buildings, cannot produce biomass by water. After group discussions, we think there are two reasons. One is that the estimated accuracy of the land cover map leads to the biomass production in an irrigated area classified as Buildup area. Another is that the plants in the urban area produce biomass(*Ibrahim*, 2012). The biomass productions were collected from plants include grasses, shrubs, trees etc., planted in the urban area in Miandoab.

4.6 Table of contribution

This assignment was completed by the efforts of the whole team. Group 1 members actively produced maps, raised great suggestions and completed the writing of the group report. The contribution of this assignment for each member is the same. Of course, there is a good task assignment, as shown in table 9.

Table 9 *Table of contribution*

Group Member	Contribution
Aditya Vikram Jain	Writing discussion part and image processing
Zhang, Fengbo	Writing discussion part and image processing
Luis Felipe Sierra Ponguta	Writing methodology part and image processing
Sintayehu Fetene Demessie	Writing results part and image processing
Kiggundu Hadar	Writing introduction part and image processing
Natalia Cárdenas Niño	Writing results part and image processing
Juan Bernal	Writing results part and image processing

5. REFERENCES

1. Bakhshianlamouki, E., et al. (2020), A system dynamics model to quantify the impacts of restoration measures on the water-energy-food nexus in the Urmia lake Basin, Iran, *Science of The Total Environment*, *708*, 134874.
2. Bastiaanssen, W. G., et al. (1998), A remote sensing surface energy balance algorithm for land (SEBAL). 1. Formulation, *Journal of hydrology*, *212*, 198-212.
3. Grosso, C., et al. (2018), Mapping maise evapotranspiration at field scale using SEBAL: A comparison with the FAO method and soil-plant model simulations, *Remote Sensing*, *10*(9), 1452.
4. Hesami, A., and A. Amini (2016), Changes in irrigated land and agricultural water use in the Lake Urmia basin, *Lake and Reservoir Management*, *32*(3), 288-296.
5. Ibrahim, E. S. (2012), *Biomass potentials for bioenergy production from build-up areas*, University of Twente Faculty of Geo-Information and Earth Observation (ITC).

6. WWO (2020), Miandoab Monthly Climate Averages, *Retrieved from* *https://www.worldweatheronline.com/miandoab-weather-averages/mazandaran/ir.aspx*.